Industrial Health 2007, **45**, 199–208 **Original Article**

Effects of Sash Movement and Walk-bys on Aerodynamics and Contaminant Leakage of Laboratory Fume Cupboards

Li-Ching TSENG[1], Rong Fung HUANG[2]*, Chih-Chieh CHEN[1] and Cheng-Ping CHANG[3]

[1] Institute of Occupational Medicine and Industrial Hygiene, National Taiwan University, 1 Jen-Ai Rd., Sec. 1, Taipei, Taiwan

[2] Department of Mechanical Engineering, National Taiwan University of Science and Technology, 43 Keelung Road, Section 4, Taipei, Taiwan

[3] Institute of Occupational Safety and Health, Council of Labor Affairs, 99 Lane 407, Hengke Rd., Sijhih City, Taipei, Taiwan

Received March 29, 2006 and accepted August 30, 2006

Abstract: In order to speculate the physical mechanisms of contaminant leakage during sash movement and walk-bys through a laboratory fume cupboard, the complicated three-dimensional flow patterns and the real-time tracer gas leakage are studied via the laser-assisted flow visualization method and the standard gas sampling technique, respectively, over a transparent, full scale chemical fume cupboard. Through the flow visualization, the evolution of drastic changes of the flow pattern is demonstrated. The highly turbulent jet-like currents are induced by the unsteady flow motion near the cupboard face. Large-scale turbulent eddies accompanied with the jet-like currents obviously bring large amount of in-cupboard smoke out to the atmosphere. The turbulent mixing extends the size and the strength of the large-scale eddy circulations, and predominantly contributes to the mechanism that causes the severe spread of contaminant leakage in few seconds. The tracer gas tests that are conducted by employing pr-EN 14175:2003 method show consistent containment results with the flow visualization findings. The temporally evolving large-scale turbulent eddies induced by the sash movement and the walk-bys cause substantially high contaminant leakage to the environment and the breathing zone of the operator.

Key words: Laboratory fume cupboard, Tracer gas, Flow visualization, Vortex, Turbulent dispersion

Introduction

Laboratory fume cupboards are the first defense to minimize chemical exposure to research workers. They are considered the primary means of protection from inhalation of hazardous gases, fumes, vapors, and particulate matter generated inside the enclosure. The performance of a fume cupboard is determined by a complex interaction of factors, such as the fume cupboard geometry, suction flow rate, sash opening height, etc. Besides, the unwanted air currents outside the sash opening can lead to disruptive cross drafts across the face of the cupboard. Some of these cross drafts are a consequence of natural phenomena and some are induced by the transit and actions of laboratory personnel, such as rapidly sash opening and people walk by. The results of previous researches indicate that the temporal variability induced by the cross drafts will cause some increased contaminant outbreaks[1–6].

The previous studies[7–11] suggest that maintaining a specific face velocity would not guarantee that a fume cupboard could perform high containment efficiency because no correlation between the face velocity and the performance was observed.

*To whom correspondence should be addressed.

The proposed fume cupboard testing protocol, prEN 14175-3:2003 "Fume Cupboards Part 3: Type Test Methods"[12], incorporates a dynamic sash movement test and a robustness test that indicate the performance of fume cupboards to contain fumes when subjected to external draughts. This test protocol requires that measurements of tracer gas concentration involved in conducting rapidly sash movement at a constant rate and moving a large plate horizontally in front of the fume cupboard to create a draught for simulating a person walking by.

In this study, flow visualization is conducted to examine the effect of sash movement and walk-bys on the flow patterns of the fume cupboard. The tracer gas measurements by following the prEN 14175-3:2003 method are subsequently conducted to verify the correlation of the flow patterns and the contaminant leakage of a laboratory fume cupboard. The purposes are to reveal the physical mechanism of the dynamic factors affecting the containment, to compare the flow visualization results with the prEN 14175-3:2003 tracer gas measurement, and to find the design parameters of fume cupboards.

Materials and Methods

The test fume cupboard is shown in Fig. 1. It has an 850 mm × 1,200 mm aperture, which is made of transparent acrylic plates so that the laser beams can pass through for flow visualization. An AC motor/centrifugal fan provides the suction of the hood. The suction flow rate is measured by a venturi flowmeter along with a calibrated pressure gauge. Measurement is conducted with the sash at a height of 500 mm. The operating suction flow rate is 0.36 m^3/s so that the face velocity at 50 cm sash opening is about 0.5 m/s. The error of the suction flow rate measurement is less than 1% of the reading.

Experiments are carried out in a well-controlled test room. During the experiment, turbulence and external interference from external sources such as the air supply diffusers, doors, and traffic in the room are restricted.

The experimental study includes two parts: (1) flow visualization, (2) tracer gas test.

Flow visualization

The experimental apparatus for flow visualization is shown in Fig. 2. A paraffin oil mist is produced in the smoke generator and continuously seeded through the homemade smoke ejectors into the test section. The diameter of the oil-mist particles, measured by a Malvern 2600C particle analyzer, is 1.7 ± 0.2 μm. The density of this particle is 0.821 g/ml. Without considering the effect of turbulent diffusion, the relaxation time constant is estimated to be less than 7.7×10^{-5} s and the Stokes number is in the order of 10^{-6} within the range of experiment. Therefore, Flagan and Seinfeld[13] suggest that the seeded particles can properly follow the flow fluctuations at least up to 10 kHz.

For simulating the contaminant transport process, the streams of the smoke are generated from the smoke generator and piped to the smoke ejector. The smoke is distributed through a wire mesh outlet diffuser. The laser beam from Nd:YAG laser is transmitted through an optical fiber and connected to a 20° laser-light sheet expander. The laser-light sheet expander is mounted on an adjustable block so that the light sheet can be easily aligned on different planes. The laser-light sheet is adjusted to a thickness of about 0.5 mm. A Hi-8 CCD camera is used to record the particle images. The camera is equipped with an asynchronous variable electronic shutter (ranging from 1/12,000 to 1/60 s) and could record images at 30 fps.

The visualization experiments are conducted in the following procedures:

1) Visualization on the effect of sash movement

The arrangement of the smoke ejectors and the release rate of the smoke are in accordance with the sash movement test of the prEN 14175-3:2003 protocol. The release rate of the smoke was 4.5 L/min. Nine smoke gas injectors are positioned inside the cupboard on the plane 200 mm away from the plane of sash. The 9 smoke injectors are fixed in the grids formed by the intersection of the following lines: (1) three equally spaced vertical lines between the two extreme side boundaries of the sash opening with the two outermost lines 100 mm from the two extreme side boundaries; (2) three horizontal lines with the bottom line 100 mm, the middle line 250 mm and the top line 650 mm above the bottom horizontal boundary of the sash opening. The smoke is released into the cupboard for 360 s. Then, the sash is closed rapidly within 1 s. After a period of 240 s, the sash is quickly opened within 1 s. The smoke is then recorded for 780 s.

The operator standing in front of the hood opening usually would induce a recirculation wake because the human body behaves like a bluff-body when he/she stands in a crossflow[14, 15]. In the neighborhood of the base of a three-dimensional bluff body an adverse pressure gradient will be produced as a result of reverse flow by an obstacle. In order to observe the effects of the operator's presence on the flow structure, experiments with a manikin standing in front of the cupboard are also performed. The manikin's vertical centerline is in

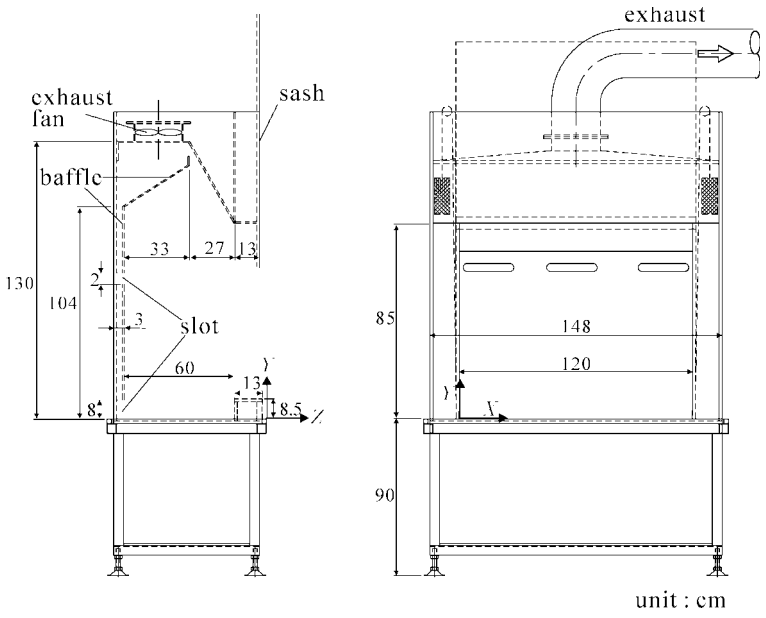

Fig. 1. Experimental setup.

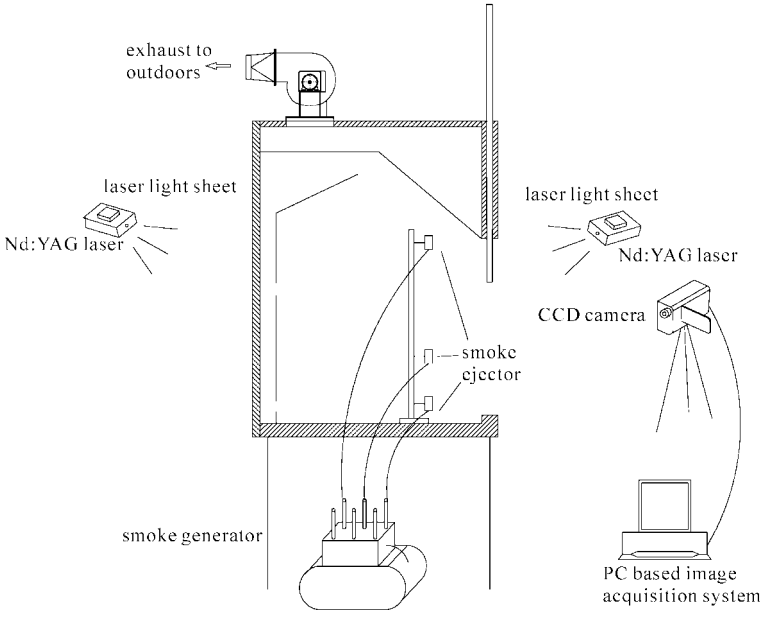

Fig. 2. Experimental apparatus for flow visualization.

line with the vertical centerline of the cupboard. The distance between the nose tip of the manikin and the cupboard opening is 75 mm.

2) Visualization on the effect of walk-bys

The release rate and the arrangement of the smoke ejectors are arranged in the same way as sash movement arrangement. As shown in Fig. 3, the plate is mounted upright and perpendicular to the plane of the sash, 200 mm above the floor, and 400 mm from the farthest part of the plane of the sash. The plate is moved with a speed of 1.0 m/s backward and forward across the face of the fume cupboard. The traverse of the plate is extended for 600 mm on each side beyond the width of the cupboard. The time between each traverse is 30 s. Six traverses are completed in each test.

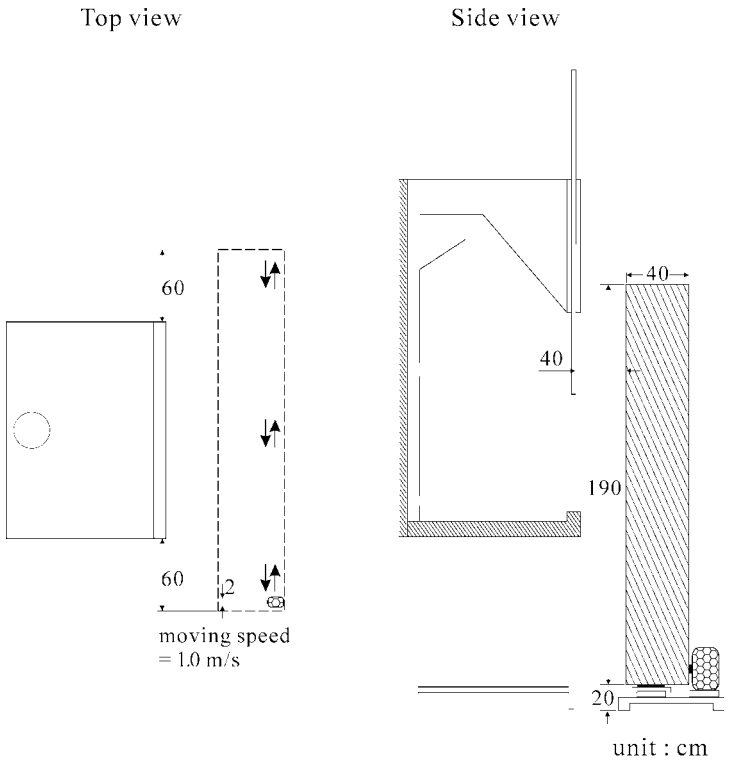

Fig. 3. Experimental apparatus for walk-by test.

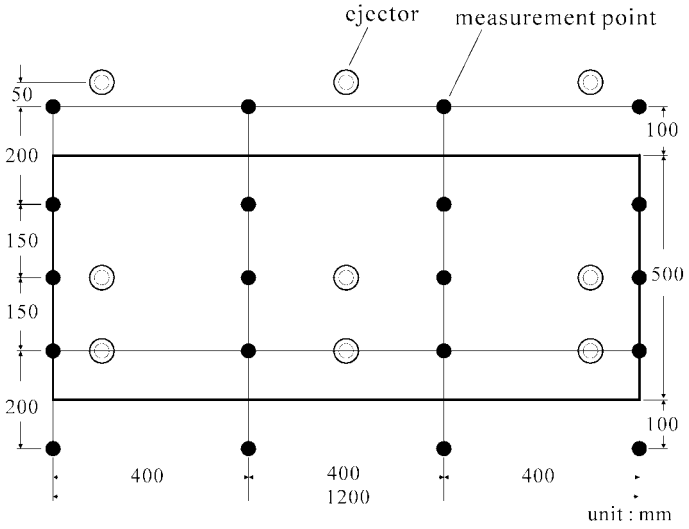

Fig. 4. Sampling grid and source position arrangements by employing dynamic containment test of pr-EN 14175:2003 method.

Tracer gas test

The tracer gas measurements are conducted in accordance with the prEN 14175-3:2003 protocol by using 10% SF_6 in nitrogen gas (N_2) as the tracer gas. The release rate of the SF_6 is 4.5 L/min. Twenty sampling probes are positioned at the grids (the black dots) on the rectangular area in the measurement plane, as shown in Fig. 4. Tracer gas samples are taken through a stainless steel tube of 10 mm internal diameter at a suction velocity 14.9 cm/s at the inlet. The distance between the measurement plane of the tracer gas

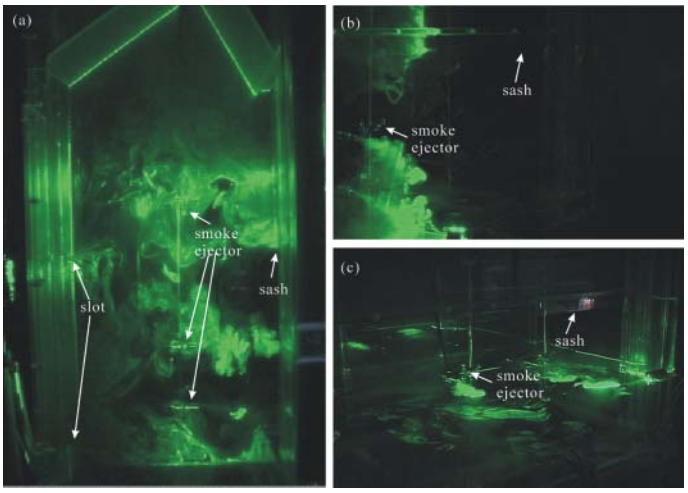

Fig. 5. Side view of smoke patterns during the initial static condition.
(a) inside cupboard, (b) at vertical plane of cupboard face, (c) at horizontal plane of cupboard face.

and the cupboard opening is 50 mm. The SF_6 concentrations are measured and recorded with the SapphIRe™ Infrared Analyzer. The lower and upper detection limits for SF_6 using this instrument are 0.001 ppm and 100 ppm, respectively. The sampling flow rate is 14 l/min. The accuracy of the instrument is 10% of the reading for concentrations between 0 and 1 ppm, 20% of the reading between 1 and 4 ppm. The sampling rate of the detection is 20 readings per second. Average value over 1 s is recorded so that the recorded data rate is 1 Hz.

1) Dynamic sash movement test following the prEN 14175-3:2003 protocol

The arrangement of the tracer gas ejector and the procedure of the sash movement are arranged in the flow visualization arrangement.

Another tracer gas experiment that a manikin placed in front of the cupboard is conducted. Tracer gas samples are taken through a stainless steel tube of 13 mm internal diameter that the suction velocity is 175.8 cm/s. The detector probe is fixed in a position touching the nose tip of the manikin in the region of the breathing zone, with the center of the probe 660 mm above the work surface and 20 mm in front of the sash. The distance between the nose tip of the manikin and the cupboard opening is 75 mm.

2) Dynamic walk-bys test following the prEN 14175-3:2003 protocol

The positions of the tracer gas ejector, the procedures of the walk-by test are arranged in the same way as the flow visualization section. The arrangement of the sampling probes and the suction rate is the same as the sash movement test.

Results and Discussion

Effect of sash movement on flow structure and contaminant leakage

1) Flow visualization

i) Initial static condition

During the period of initial static time before sash movement, one large, unsteady, three-dimensional recirculation zone appears behind the sash plane at the upper-aperture height across the work surface is observed, as shown in Fig. 5(a). The large-scale vortex structures are found around the side walls and the doorsill of the cupboard as shown in Figs. 5(b) and (c). It is postulated that these recirculation zones are the result of turbulent flow separation. The boundary layer is forced to separate from the plane wall and the vortices are induced and stretched around near the bottom and side walls of the cupboard. Roll ups of the contaminant near these regions may severely contribute to the contaminant leakage.

ii) As the sash is rapidly closed

Rapidly closing the sash would enlarge the mass of the upper recirculation zone across the work surface, as shown in Fig. 6(a). Due to the enough negative pressure induced by the continuous suction effect in the cabinet, the upper recirculation zone is trapped and caused a downward rotation.

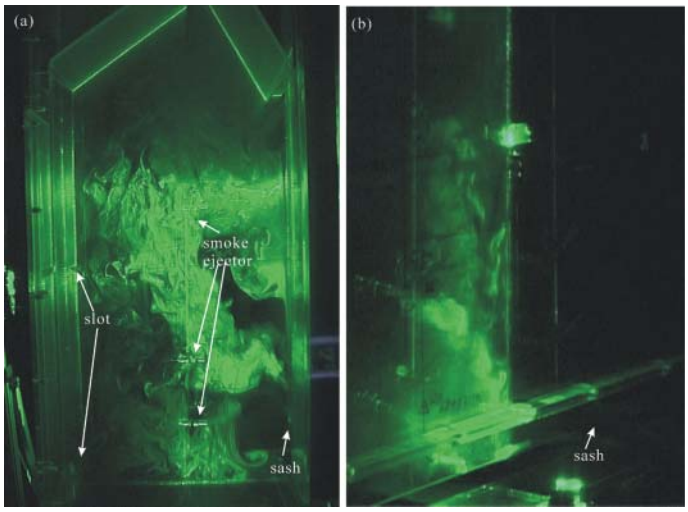

Fig. 6. Side view of smoke patterns when sash is closed.
(a) inside cupboard, (b) at vertical plane of cupboard face.

The rotational flow structures are even more intense and the magnitude of the velocities is higher, resulting in a powerful dynamic turbulent mixing. As we observe the face of the cupboard, the sweep effect is observed as shown in Fig. 6(b). The large-scale recirculation zone originally occurred near the doorsill almost disappears.

iii) As the sash is rapidly opened

At the moment of the sash opening, the flow structures evolve in four stages: formation, development, propagation and decaying of turbulent jet-like flow, as shown in Fig. 7. The streak pictures of the flow evolution on the symmetry plane are shown in Figs. 7(a)–(d). In the "formation" stage, when the sash is just opened, the smoke in the cabinet pushed by the air currents rushing into the cabinet turns around when it meets the vortex rotating behind the sash. The vortex behind the sash is induced by the up-shear effect due to the opening movement of sash. The outward going current forms a jet-like flow and ejects across the sash plane to the atmosphere, as shown in Fig. 7(a). As the time evolves in the development stage, the jet-like flow disperses forward and downward so that the region covered by the smoke enlarges as shown in Fig. 7(b). The coherent jet-like flow keeps expanding and dispersing and finally the lower boundary of the outward flow touches the doorsill, as shown in Fig. 7(c). Flows in this stage denoted as propagation. Eventually, the wave front of the ejecting jet-like flow losses momentum and disperses to the whole field outside the sash plane through the mechanism of turbulent diffusion, as shown in Fig. 7(d). The flow in this stage is in decaying. The evolution process of the turbulent eddies during the sash opening is completed in about 20 s. The flows on the horizontal plane evolving from Fig. 7(e)–(h) show corresponding process of the contaminant leakage corresponding to the four steps of Fig. 7(a)–(d). It is particularly notable that the creation of turbulent jet-like flow may carry large amount of the pollutant-laden smoke out of the cupboard and disperses into the breathing zone of the operator, as shown in Fig. 8.

2) Tracer gas test

As shown in Fig. 9, the SF_6 concentration declines to the nearly baseline level following the sash closed. As the sash opens, a large-peak pattern of SF_6 concentration due to the ejection and dispersion of the jet-like flow as demonstrated in Fig. 7 is recognized. It is postulated that the large-scale vortex structures occurring across the sash opening concur with the high degree of contaminant leakage in those areas, served to reveal the essential features of the contaminant transport process. The values of SF_6 concentration subjected to this temporal movement are not significantly higher than those of the initial condition (before sash opens) may be because that the measured SF_6 concentrations, according to the prEN 14175-3:2003 method, are the "bulk samples" over the entire multiple grids on the cupboard face. From the visual test, it is known that the scaling of the large-scale eddy structure before and after the sash opened are approximately the same in this case.

The tracer gas experimental results demonstrated in Fig. 10 show that the values of SF_6 concentration around the

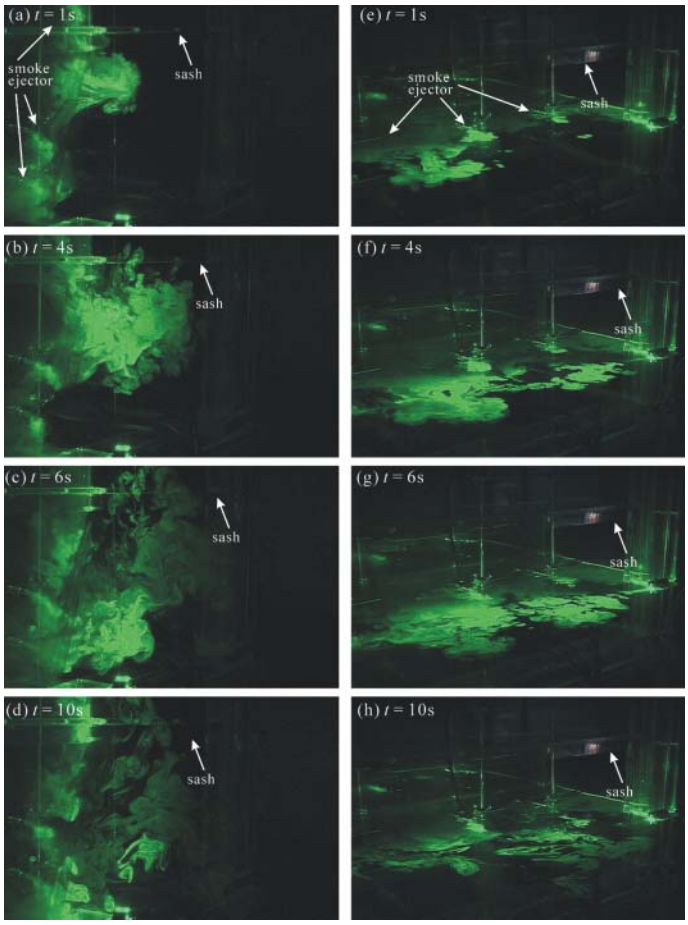

Fig. 7. Evolution of flow pattern after sash opens, at vertical plane of (a) formation stage, (b) development stage, (c) propagation stage, (d) decaying stage; at horizontal plane of (e) formation stage, (f) development stage, (g) propagation stage, (h) decaying stage.

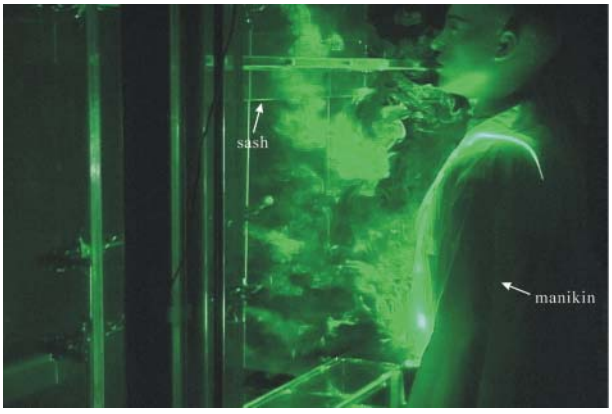

Fig. 8. Smoke patterns around breathing-zone of manikin after sash opens.

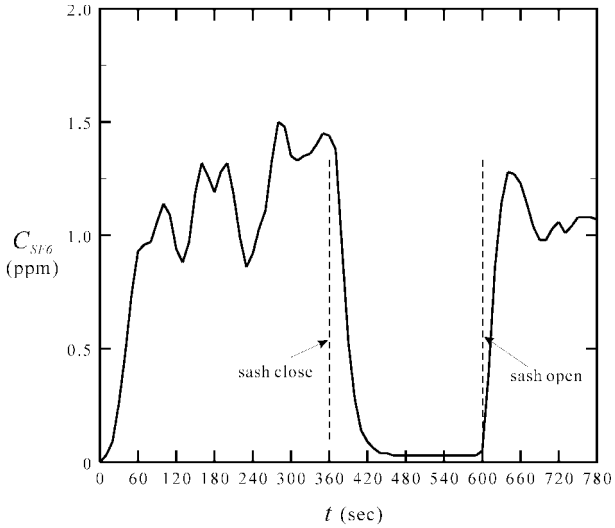

Fig. 9. Time histograms of SF_6 leakages during sash movement by employing pr-EN 14175-3:2003 method.

breathing zone of the manikin reach the peak value by the time the sash opens. The deviation of Fig. 10 from Fig. 9 may be because that the bulk SF_6 sample measured by following the prEN 14175-3:2003 method is hardly to represent the variation between each individual region of the cupboard. It is greatly possible that the measured tracer gas concentration may be underestimated in certain severe leakage areas due to "averaging". This situation is particularly important in the evaluation of the release of contaminant at the breathing zone of the manikin where high impacts on a short time scale may be extremely dangerous.

Effect of walk-bys on the flow structure and contaminant leakage

1) Flow visualization

A plate moving rapidly in front of the cupboard is used to simulate air currents caused by the people walk by in front of the cupboard. At the stage of forward movement of the

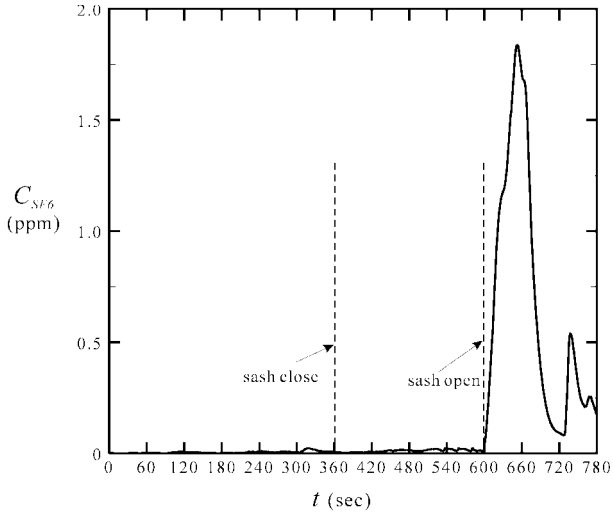

Fig. 10. Time histogram of SF_6 leakages in the breathing-zone of manikin during sash movement.

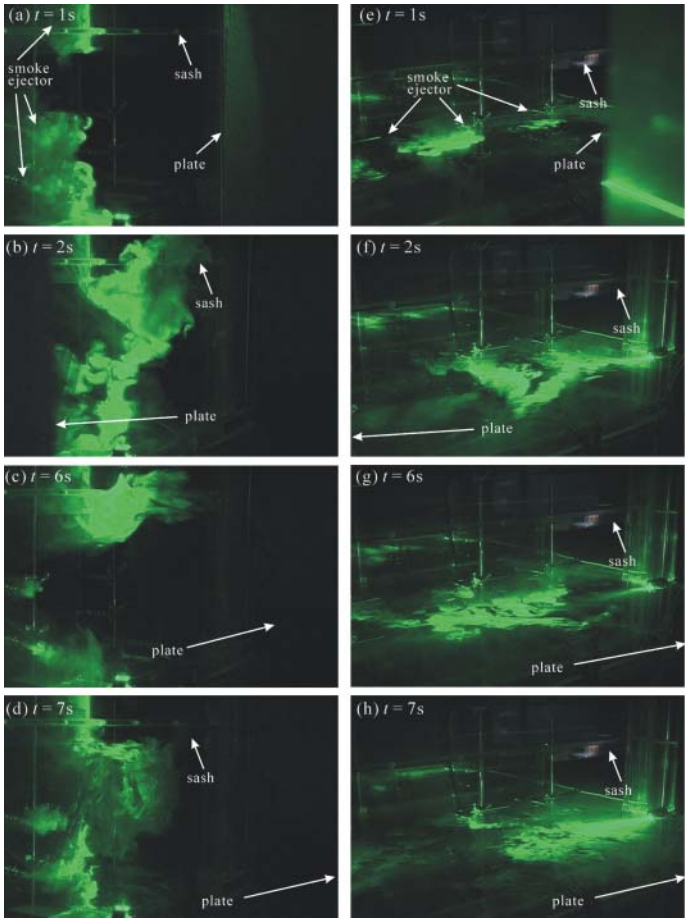

Fig. 11. Evolution of flow patterns during walk-by test, at vertical plane of (a) 1st sec, (b) 2nd sec, (c) 6th sec, (d) 6th sec; at horizontal plane of (e) 1st sec, (f) 2nd sec, (g) 6th sec, (h) 7th sec after starting of plate traveling.

plate, additional turbulence is introduced, the sweep effect is obvious. The high pressure region formed in the front of the plate pushes fresh air into the relatively negative pressure region of the interior of the cupboard. A considerable-size air cavity is formed at the first second of the forward movement of the plate, as shown in Fig. 11(a). As the plate passes by, the wake region behind the plate has low pressure and high turbulence. A high-velocity smoke stream disperses rapidly and rushes out in an unstable elliptical roll, as shown in Fig. 11(b). The size of the large-scale turbulent eddies is dramatically enlarged that the contaminants originally inside the cupboard may reach significant potential to escape. If a manikin is placed in front of the cupboard, it's observed that the cross draft induced by the walk-bys may easily sweep contaminants from the working area into the operator's breathing zone, as shown in Fig. 12.

At the stage of the backward movement of the plate, the cross drafts drastically alter the shape and the extent of the turbulent eddies. The air in the middle levels is pushed by the positive pressure formed in the front of the plate and rushes into the cabinet to form cavitations. A jet-like flow under the sash is induced by the up-shear effect as shown in Fig. 11(c). The jet-like flow disperses and spreads out throughout the cupboard face due to the downward turbulent diffusion, as shown in Fig. 11(d). The turbulent diffusion process extends the size and the strength of the large-scale eddy circulations, and predominantly contributes to the mechanism that causes the severe spread of contaminant leakage. The dynamic evolution of the unstable large-scale turbulence is completed in about 30 s. The flow evolution on the horizontal plane from Figs. 11(e)–(h) shows the contaminant spreading process corresponding to the Figs. 11(a)–(d).

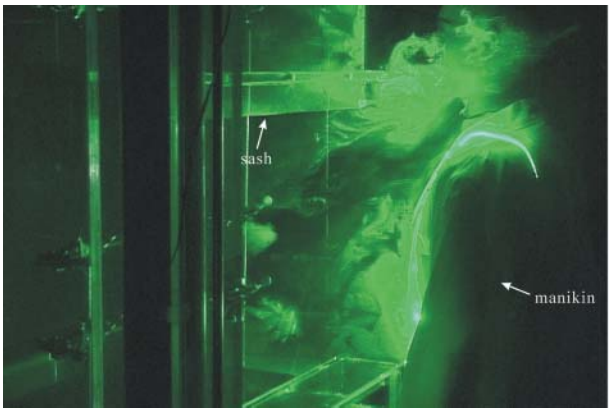

Fig. 12. Smoke patterns around breathing-zone of manikin during walk-bys.

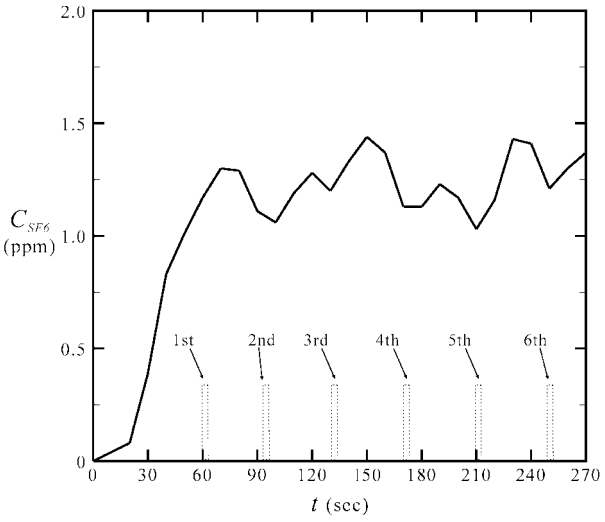

Fig. 13. Time histogram of SF_6 leakages during walk-bys by employing pr-EN 14175-3:2003 method.

2) Tracer gas test

Six periodic larger peaks of SF_6 leakage are observed due to the turbulent dispersion induced by the six traverses of the plate, as shown in Fig. 13. Each peak value of SF_6 concentration occurs on the curve at the time when the plate passes by. The large-scale turbulent eddies entrains the contaminant, resulting in regions of relatively high concentration. These regions fluctuate both in size of the turbulent eddies and the concentration of the contaminant.

As shown in Fig. 14. Six substantial larger-peak patterns of SF_6 concentration in the breathing zone due to six periodic walk-bys are recognized. The peak values of SF_6 leakage measured are nearly 20 to 50-fold higher than those of the initial static condition. It is apparent that the six peak values of SF_6 concentration due to larger-scale turbulent structures affected and is especially prevalent in the situation while an operator standing in front of the cupboard.

Conclusions

The evolution of dramatic changes of the flow patterns due to sash movement and walk-by effects are demonstrated in this study. The results of the flow visualization and the tracer gas experiment establish the fact that large-scale turbulent vortices occurring near the face of the cupboard could induce strong turbulence and therefore enhance dispersion of the recirculated contaminant, predominantly contributes to the mechanism that causes the severe spread of contaminant leakage. In view of the transient nature of

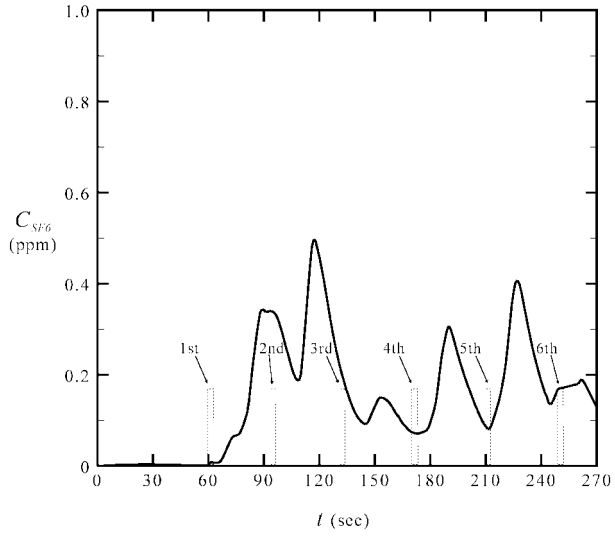

Fig. 14. Time histogram of SF_6 leakages in the breathing-zone of the manikin during walk-bys.

contaminant leakage from the fume cupboard, the ability of laboratory fume cupboards to provide protection for the worker at the face of cupboard can be strongly influenced by the temporal variability of the turbulent vortices. The effects of the sash movement and walk-bys on the containment are apparently pronounced and should be investigated thoroughly for each individual fume cupboard. Better design of the fume cupboard in preventing the creation of turbulent eddies across the cupboard face during sash movement and walk-bys should be also attempted. For example, support air system may be effective in preventing contaminants leakage.

A limitation of the sash movement and the walk-by (robustness) tests of the pr-EN 14175-3:2003 protocol is that it does not fully represent the contaminant leakage at each individual location and warrants further study. This is especially important in determining if contaminant leakages occur at the breathing zone of the operator in front of the fume cupboard, even an extremely small amount of leakage may be unacceptable for highly toxic material.

Acknowledgments

This research is supported by the Ministry of Education of Taiwan. R.O.C. under grant number 0940081791.

References

1) Caplan KJ, Knutson GW (1978) Laboratory fume hoods: influence of room air supply. Am Ind Hyg Assoc J **43**, 738–46.
2) Durst F, Pereira JCF (1991) Experimental and numerical investigations of the performance of fume cupboards. Building and Environment **26**, 153–64.
3) Altemose BA, Flynn MR, Sprankle J (1998) Application of a tracer gas challenge with a human subject to investigate factor affecting the performance of laboratory fume hoods. Am Ind Hyg Assoc J **59**, 321–7.
4) Joao RV, Party E, Gershey EL (1998) Fume hood performance: using a bypass in variable air volume systems. Appl Occup Environ Hyg **13**, 708–12.
5) Greenley PL, Billings CE, DiBerardinis LJ, Edwards RW, Barkley WE (2000) Containment testing of laboratory hoods in the as-used condition. Appl Occup Environ Hyg **15**, 209–16.
6) Ekberg LE, Melin J (2000) Required response time for variable air volume fume hood controller. Ann Occup Hyg **44**, 143–50.
7) Ivany RE, First MW, Diberardinis LJ (1989) A new method for quantitative, in-Use testing of laboratory fume hoods. Am Ind Hyg Assoc J **50**, 275–80.
8) Fletcher B, Johnson AE (1992) Containment testing of fume cupboards-I. Methods. Ann Occup Hyg **36**, 239–52.
9) Fletcher B, Johnson AE (1992) Containment testing of fume cupboards-II. Test room measurements. Ann Occup Hyg **36**, 395–405.
10) Volin CE, Joao RV, Reiman JS, Party E, Gershey EL (1998) Fume hood performance: face velocity variability inconsistent air volume systems. Appl Occup Environ Hyg **13**, 656–62.
11) Maupins K, Hitchings DT (1998) Reducing employee exposure potential using the ANSI/ASHRAE 110 method of testing performance of laboratory fume hoods as a diagnostic tool. Am Ind Hyg Assoc J **59**, 133–8.
12) CEN (2003) Fume Cupboards—Parts 3: Type test methods, European Committee for Standardization (prEN 14175-3).
13) Flagan RC, Seinfeld JH (1988) Fundamentals of Air Pollution Engineering, 290-357, Prentice Hall, Englewood Cliffs, New Jersey.
14) Kim T, Flynn MR (1992) The effect of contaminant source momentum on a worker's breathing zone concentration in a uniform freestream. Am Ind Hyg Assoc J **53**, 757–66.
15) Flynn MR, Ljungqvist B (1995) A review of wake effects on worker exposure. Ann Occup Hyg **39**, 211–21.